

LUT-Based Transmit Mode Calibration Complexity Reduction Method for Wireless Power Transfer

Young-seok Lee

Dept. of ECE, Seoul Nat'l University
Seoul, South Korea
ryanlee@snu.ac.kr

Taeyeong Yoon

Dept. of ECE, Seoul Nat'l University
Seoul, South Korea
taeyeong.yoon@snu.ac.kr

Sanghun Lee

Dept. of ECE, Seoul Nat'l University
Seoul, South Korea
sanghun8.lee@snu.ac.kr

Minje Kim

Dept. of ECE, Seoul Nat'l University
Seoul, South Korea
sbi06035@snu.ac.kr

Jaesup Lee

Samsung Advanced Institute of Technology
Suwon, South Korea
jaesup2003.lee@samsung.com

Jungseuk Oh

Dept. of ECE, Seoul Nat'l University
Seoul, South Korea
jungseuk@snu.ac.kr

Sangwook Nam

Dept. of ECE, Seoul Nat'l University
Seoul, South Korea
snam@snu.ac.kr

Abstract—This paper introduces a calibration method for transmitter arrays for the power transmit mode in wireless power transfer (WPT) systems. Focusing on the challenges posed by non-uniform power distribution in large array antenna systems, we propose a technique adaptable to various power distribution designs. Our method also simplifies the calibration process, making it feasible for real-world applications with large array antennas. The paper validates our methodology, from the hardware system to experimental results, demonstrating the effectiveness of our approach by transmitting CVX optimized radiation patterns. The receiver array achieved received RF power of 3.57 Watts at 0.5 meters.

Index Terms—Array calibration, Convex optimization, IoT device, Large array antenna, Wireless power transfer

I. INTRODUCTION

As RF technology in Wireless Power Transfer (WPT) advances, the need for large array antenna systems increases. This trend highlights the importance of transmitter antenna calibration processes. Understanding the expected transmit patterns emitted by the transmit antenna is essential for effectively transmitting desired amplitude and phase patterns.

Most WPT calibration procedures draw from methods developed for large array RADARs. Reference [1] have well-organized these methods. The Rotating Element Electric Field (REV), introduced in [2], measures amplitude variations of the array's electric field as each antenna element's phase changes. Subsequently, REV methods without phase measurement were introduced [3], along with reduced complexity versions [4]-[5]. Also, the Multi-Element Phase Toggle (MEP) method is detailed in [1] and [6]. These methods have been commonly used until now for WPT calibrations by conventional techniques.

This paper introduces a method for calibrating transmitter arrays in WPT power transmit mode. Our approach streamlines

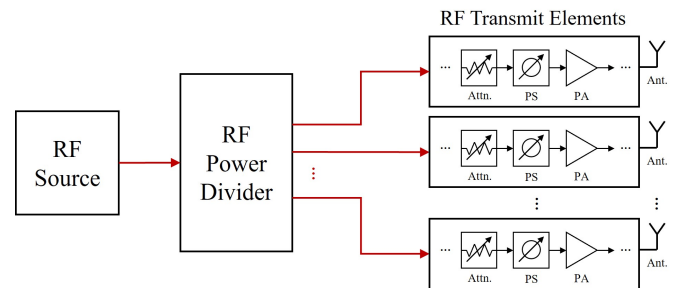


Fig. 1. WPT transmitter RF module architecture. Note that Attn., PS, PA are the Attenuator, Phase Shifter, and Power Amplifier, respectively.

the calibration process for effective application in real systems. We organize this novel method systematically, incorporating our unique topology. The structure of this paper is as follows: Section II presents our proposed algorithm and its methodology. Section III provides an overview of the hardware system we developed, along with its measured results. Finally, Section IV offers the conclusions.

II. CALIBRATION TOPOLOGY

A. Calibration Scenarios

Figure 1 depicts the transmitter topology common to many contemporary RF-WPT systems. The RF source generates a signal that is then distributed by an RF power divider to each Transmit Element (TE). Each TE is equipped with digitally controllable attenuators and phase shifters, allowing for precise manipulation of each signal's amplitude and phase. Research on power divider designs, including parallel and cascaded feeding topologies, is varied [7]-[9]. Our proposed algorithm

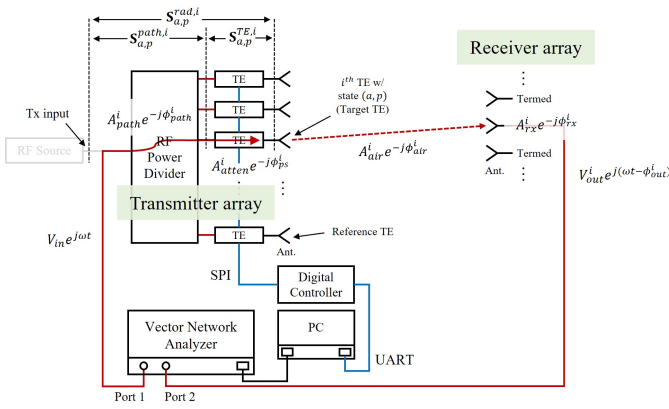


Fig. 2. Block diagram of proposed calibration setup and signal marks at each stages. RF lines are marked in red, digital lines in blue.

is adaptable, and designed to be effective regardless of the feeding network type, also including the mismatches of from the power divider fabrications.

In an ideal setup, an RF power divider would uniformly distribute power to all TEs, but real-world systems commonly experience uneven distribution. Such uneven distribution complicates the calibration process.

Ideally, uniform power distribution would greatly ease calibration. By individually measuring several TE's amplitude and phase changes, signal characteristics could be easily predicted and adjusted. However, the extent of deviation from uniform distribution can be significant, varying with system types. In cases where the difference is substantial and beyond approximation, it becomes imperative to consider the entire line from the RF source to the TE endpoint for accurate analysis. This non-uniformity poses a greater challenge in systems with a larger number of TEs. Manually measuring and compensating each port of the RF power divider becomes a task, demanding considerable resources and time.

Our proposed calibration process aims to accurately acquire amplitude and phase information of signals radiated from each TE, based on the settings of the attenuators and phase shifters. The approach of our calibration methodology lies in two key aspects:

- Streamlined Calibration: Our method enables the calibration in a single session, eliminating the need to modify the measurement setups.
- Reduction Techniques: The proposed calibration process maintains accuracy while substantially increasing the speed of the operation.

B. Channel-model Based Calibration Methodology

Consider a conventional WPT system comprising a phased array transmitter with M elements. This system uniquely allows independent control over the amplitude and phase of each TE. While the receiver can be any antenna, the inherent design of the WPT system facilitates its use as a receiver. Figure 2 illustrates the calibration setup for this system. Here, the RF source is isolated from the transmitter, and instead, Port

1 of the Vector Network Analyzer (VNA) is connected. All TEs are linked via digital lines and managed through a PC. The receiver antenna is attached to Port 2 of the VNA; however, only one antenna is active, with the others being terminated. Notably, the PC and VNA are interconnected through various communication protocols (such as General Purpose Interface Bus (GPIB), Local Area Network (LAN), and Universal Asynchronous Receiver/Transmitter (UART)), allowing for the straightforward measurement of S -parameters. It's important to note that our calibration method is adaptable to any hardware configuration, as long as the TEs are controllable and the VNA is digitally linked to the PC.

Since our objective is to estimate the amplitude and phase characteristics at each TE in our WPT system, it is crucial to understand the signal path from the VNA to i^{th} antenna to the receiver. Let's consider the scenario where a signal $V_{in}e^{j\omega t}$ is generated by the VNA. Here, ω represents the operational frequency of the system, which is typically single frequency in WPT systems. Specific state of attenuator and phase shifter is digitally entered at the i^{th} TE. Other TEs are in off-status while i^{th} TE is on measurement.

As this signal progresses through the system, it undergoes various path losses, such as those due to the power divider, cables, and connectors. We can mathematically represent the total channel losses encountered by the signal on its way to the i^{th} antenna as $A_{path}^i e^{-j\phi_{path}^i}$, encompassing all the signal's transformations through these components. Additionally, at each TE, the combined effect of the attenuator and phase shifter at such state is represented as $A_{atten}^i e^{-j\phi_{ps}^i}$, which adjusts the signal's amplitude and phase shift. (Precisely, all effects inside the TE are involved) As the signal propagates through the air, it experiences further attenuation and phase delay, expressed as $A_{air}^i e^{-j\phi_{air}^i}$. Finally, additional losses occur in the receiver, represented as $A_{rx}^i e^{-j\phi_{rx}^i}$. All these expressions are scaled in terms of voltage ratios (V/V).

If we measure S_{21} of single state by VNA, it can be expressed by combining all the path losses described above:

$$S_{a,p}^i = A_{path}^i A_{atten}^i A_{air}^i A_{rx}^i e^{-j(\phi_{path}^i + \phi_{ps}^i + \phi_{air}^i + \phi_{rx}^i)} \quad (1)$$

where $S_{a,p}^i$ represents the complex value of S_{21} measured by the VNA under a specific state of the attenuator and phase shifter (a, p). By dividing $S_{a,p}^i$ by the channel factors of air and receiver, we can deduce the channel between the input of the transmitter array (Tx input) and the i^{th} element. This deduced channel, denoted as $C_{a,p}^i$, is a complex value and can be expressed as follows:

$$C_{a,p}^i = \frac{S_{a,p}^i}{A_{air}^i e^{-j\phi_{air}^i} \cdot A_{rx}^i e^{-j\phi_{rx}^i}} \quad (2)$$

here, the channel effects in the air can be ideally calculated using the Friis equation [10], which is formulated as:

$$A_{air}^i = \sqrt{G_t G_r} \cdot \frac{\lambda}{4\pi R}, \phi_{air}^i \equiv \text{mod}(k \cdot R, 2\pi) \quad (3)$$

where G_t and G_r represent the linear scale antenna gains of the transmitter and receiver antennas, respectively, R is the distance between the two antennas, and k is the wave number. Since our goal is to estimate the amplitude and phase at the i^{th} element, multiplying $C_{a,p}^i$ by the input power (power from the RF source) calculates the power radiating from the i^{th} element for each state. This can be expressed as:

$$R_{a,p}^i = C_{a,p}^i \cdot V_{source} e^{j\omega t} \quad (4)$$

where $R_{a,p}^i$ represents the complex value of the signal radiating from the i^{th} element at state (a, p) , and $V_{source} e^{j\omega t}$ is the signal from the RF source. By multiplying the channel with the input power, we can derive the estimated radiation power, which is the primary objective of this calibration.

By measuring S_{21} while sweeping through all desired states (a, p) and repeating this for each of the M elements, we can compile a comprehensive table. After adjusting values using equations (2)-(4), a Look-up Table (LUT) that correlates the radiated amplitude and phase for each state is generated. Algorithm 1 organizes this process.

Algorithm 1 Generation of LUT

- 1: **procedure** INITIALIZE(: Turn off all TEs.)
 - 2: Select the first TE and set the attenuator and phase shifter to the desired state, starting with 0 dB attenuation and 0-degree phase shift for maximum power. Measure $S_{a,p}^i$ (S_{21}).
 - 3: Repeat step 2 for all desired states. If using a p -bit attenuator and a q -bit phase shifter, the total combinations are 2^{pq} . Selectively choose sequences from the available options, generating a table with $a \cdot p$ rows. Selected attenuation and phase are $\{A_1^1, A_2^1, \dots, A_a^1\}$, $\{\lambda_1^1, \lambda_2^1, \dots, \lambda_p^1\}$, respectively.
 - 4: Apply step 2 for all TEs.
 - 5: Compensate the measured S_{21} values using equations (2)-(4) and calculate $R_{a,p}^i$ to create the desired LUT.
 - 6: **end procedure**
-

C. Complexity Reduction

Building the LUT using the described procedures is effective but time-consuming, especially for larger arrays. For instance, calibrating a 256-element array with standard 3-bit attenuators and 4-bit phase shifters results in a total calibration complexity of 32,512 (256×2^7). Given that this method is intended for large array antennas, significantly reducing the calibration process is crucial. Therefore, the primary goal of this reduction is to simplify the creation of LUT.

The fundamental approach to reducing complexity involves fully measuring single TE and extrapolating the findings to others. As illustrated in Figure 2, we designate the i^{th} TE as the ‘Target’ TE. When set at a state (a, p) , the total channel from the RF source to this TE is $S_{a,p}^{rad,i}$. This channel can be divided into two parts: $S_{a,p}^{path,i}$, the total channel from the RF

source to the TE’s input, and $S_{a,p}^{TE,i}$, the total channel of the target TE.

$$S_{a,p}^{rad,i} = S_{a,p}^{path,i} \times S_{a,p}^{TE,i} \quad (5)$$

Given the uniform manufacturing of TE boards, it’s reasonable to overlook minor variations between them, assuming consistent performance for simpler calibration.

$$S_{a,p}^{TE,i} \approx S_{a,p}^{TE,j} (i \neq j) \quad (6)$$

Since $S_{a,p}^{path,i}$ remains unaffected by changes in state (a, p) , it can be treated as a constant for all states and can be written as $S_{a,p}^{path,i} = S^{path,i}$. Designate a single TE as the ‘Reference’ TE and measure all $a \times p$ states for it. For arbitrary state (a^*, p^*) , the channels of both the target and reference TE can be compared as follows:

$$\frac{S_{a,p}^{rad,i}}{S_{a,p}^{rad,ref}} \approx \frac{S_{a,p}^{path,i}}{S_{a,p}^{path,ref}} = S_{i,ref}^{path} \quad (7)$$

$S_{i,ref}^{path}$ represents a constant ratio indicating the relationship between the two TEs. By applying this constant, we can extrapolate all states for the target TE from the fully measured values of the reference TE. The extension of these states is formulated using equation (5):

$$\frac{S_{a^d,p^d}^{rad,i}}{S_{a^d,p^d}^{rad,ref}} \approx \frac{S_{a^d,p^d}^{TE,i}}{S_{a^d,p^d}^{TE,ref}} = S_{i,ref}^{path} \quad (8)$$

$$\therefore S_{a^d,p^d}^{rad,i} = S_{a^d,p^d}^{rad,ref} \times S_{i,ref}^{path} \quad (9)$$

(a^d, p^d) refers to the desired state for estimation. By applying this method, full state measurements of just one reference TE and single state measurements for other TEs can create LUT. For example, in a 256-element array with same conditions previously, the complexity of this reduced method is calculated as $2^7 + (256 - 1) = 383$. This demonstrates a significant reduction in complexity compared previously.

Algorithm 2 Extension of LUT

- 1: **procedure** BEGIN
 - 2: Start from step 3 of Algorithm 1, choosing any TE as the reference, not limited to the first one.
 - 3: Select the i^{th} element (target TE) and measure only one S_{21} at state (a^*, p^*) , denoted as S_{a^*,p^*}^i .
 - 4: Apply step 2 to all $(M-1)$ TEs.
 - 5: Use equation (9) for extension and compile the LUT.
 - 6: **end procedure**
-

III. EXPERIMENTAL RESULTS

A. System Design and Implementation

A WPT hardware system, operating at 5.64 GHz with a 16×16 transmitter and a 5×7 receiver, was developed to validate the proposed calibration method. This system, depicted in Figure 2, includes TEs each controlled by individual MCUs

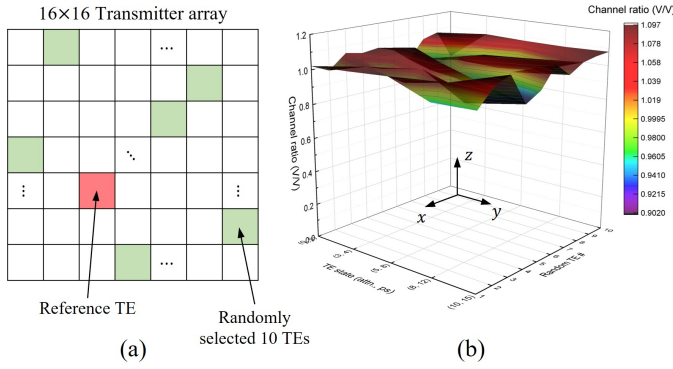


Fig. 3. Experiment of TE internal channel consistency validation; (a) randomly selected ten TEs and reference TE, (b) ratio plotting.

via SPI protocol and a PC through UART. The TE, fabricated using a commercial chip as per Figure 1, incorporates a 7-bit attenuator and a 4-bit phase shifter, with a 32 dB gain PA amplifying the signal.

The assumption at equation (6) was validated through measurement. We measured the $S_{a,p}^{TE,i}$ of the ten randomly selected TEs at five different states and checked the ratio with the reference TE. This can be written as follows:

$$C_{a,p}^{CR,i} = S_{a,p}^{TE,i} / S_{a,p}^{TE,ref} \quad (10)$$

where $C_{a,p}^{CR,i}$ is the channel ratio between reference and i^{th} TE. This result is shown at Figure 3(b), with x-axis is the randomly selected TE, y-axis is the TE state (attenuator, phase shifter), z-axis is the ratio, and it shows the ratio is distributed near 1.

B. CVX Pattern Simulation

Validation of the proposed calibration requires a specific transmit pattern, so an optimum pattern using convex (CVX) optimization was used [11]. The optimal pattern is defined as:

$$\begin{aligned} & \mathbf{max} && P_r \\ & \mathbf{subject\ to} && P_t \leq P_t^l \end{aligned} \quad (11)$$

where P_r is the total received power at the receiver, P_t is the total transmitted power, and P_t^l is the limited P_t (as constraint).

C. Measured Result

The transmitter and receiver were positioned 0.5 m apart, facing each other. The LUT was limited to 20 attenuation states and 16 phase shift states, prioritizing phase for beamfocusing and simplifying the process. A CVX pattern at 0.5 m was simulated, then incorporated into the calibration software.

Figure 4 displays the radiation pattern amplitudes as heatmaps: (a) shows the ideal CVX pattern, and (b) the actual pattern radiated in mW. We can figure out that the radiation patterns closely resemble the ideal. Figure 5 compares RF power received at the receiver in dBm, with (a) showing the simulated ideal and (b) the measured power from each array port (measured with spectrum analyzer at each ports,

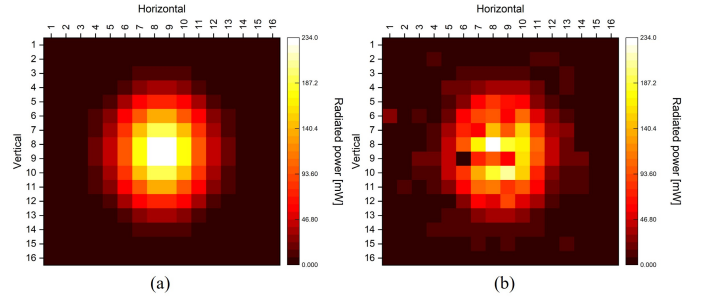


Fig. 4. Heatmap of the radiated CVX pattern at the transmitter array, in mW. It shows (a) the desired pattern and (b) the actual radiating pattern.

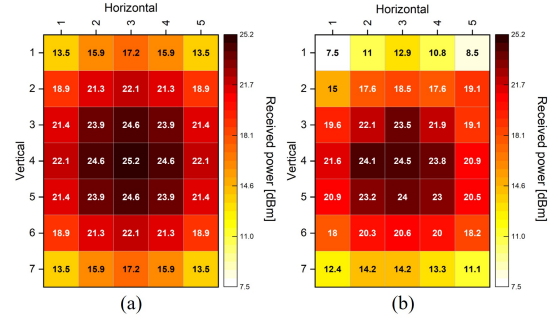


Fig. 5. Heatmap of the received power at the receiver array, measured in dBm, for the CVX pattern radiation. It shows (a) the ideally simulated power and (b) the actual measured power. The total sum of (b) was 3.57 W(RF).

respectively). The similarity between these patterns confirms the effectiveness of the calibration method, with 3.57 W of RF power at 0.5 m distance successfully received.

IV. CONCLUSION

In conclusion, this paper presented an transmit mode calibration method for WPT systems, emphasizing efficiency and accuracy. The method, utilizing a Look-up Table (LUT) and simplified measurement techniques, addresses the challenges of calibrating large array antennas. Experimental results including optimal CVX radiation patterns and RF power measurements validated the method's effectiveness, by achieving 3.57W RF power in the receiver array. The approach significantly reduces calibration complexity, proving particularly useful for large arrays. Future work could explore further improvements of accuracy, especially supporting multipath environment that includes on-line calibrations.

ACKNOWLEDGMENT

This project was funded by A-Lab., Samsung Electronics.

REFERENCES

- [1] G. Magalhães *et al.*, "A novel calibration method for phased-array radar based on element-wise time offsetting and multi-element phase toggle," *IEEE RadarConf*, Boston, MA, USA, 2019.
- [2] S. Mano and T. Katagi, "A method for measuring amplitude and phase of each radiating element of a phased array antenna," *Electron. Commun. in Japan*, vol. 65, no. 5, pp. 58–64, 1982.

- [3] I. Chiba *et al.*, "Phased array antenna calibration method in operating condition REV method," *Tech. Rep. 1, Japan Resources Observation System Organization*, 1999.
- [4] T. Takahashi, Y. Konishi, S. Makino, and H. Nakaguro, "Fast measurement technique for phased array calibration," *IEEE Trans. Antennas Propag.*, vol. 56, pp. 1888–1899, July 2008.
- [5] T. Takahashi, Y. Konishi, and I. Chiba, "A novel amplitude-only measurement method to determine element fields in phased arrays," *IEEE Trans. Antennas Propag.*, vol. 60, pp. 3222–3230, July 2012.
- [6] G. Hampson and A. Smolders, "A fast and accurate scheme for calibration of active phased-array antennas," *IEEE Antennas Propag. Soc. Int. Symp.*, vol. 2, pp. 1040–1043, 1999.
- [7] H. Koo *et al.*, "Retroreflective transceiver array using a novel calibration method based on optimum phase searching," *IEEE Trans. Ind. Electron.*, vol. 68, no. 3, pp. 2510–2520, Mar. 2021.
- [8] D. Belo, *et al.*, "A selective, tracking, and power adaptive far-field wireless power transfer system," *IEEE Trans. Microw. Theory Tech.*, vol. 67, no. 9, pp. 3856–3866, Sep. 2019.
- [9] L. Hu *et al.*, "Auto-tracking time reversal wireless power transfer system with a low-profile planar RF-channel cascaded transmitter," *IEEE Trans. Ind. Electron.*, vol. 70, no. 4, Apr. 2023.
- [10] H. T. Friis, "A note on a simple transmission formula," in *Proc. IRE*, vol. 34, no. 5, pp. 254–256, May 1946.
- [11] H.-Y. Kim, Y. Lee, and S. Nam, "Efficiency bound estimation for a practical microwave and mmWave wireless power transfer system design," *J. Electromagn. Eng. Sci.*, vol. 23, no. 1, 69–74, Jan. 2023.